These equations can be used to determine the horizontal components of $\bar{V}$, Vx_1, and Vx_2 in terms of accelerometer outputs and the desired platform torque rates. These torque rates, which must also be supplied to the gyro torquers, can be computed as follows.

Define the east, north, and vertical axes, y_1, y_2, and y_3, respectively, as in Fig. 2. The axes of y_1 and y_2 are principal directions of curvature on the ellipsoid (east and north). The components of ω_{EP} rates in principal axes are

$$\left.\begin{aligned}\omega_{y_1} &= -V_{y_2}/(\rho_m + h)\\ \omega_{y_2} &= V_{y_1}/(\rho_p + h)\end{aligned}\right\} \tag{2}$$

where

ρ_m = principal radius of curvature of the reference ellipsoid in the meridian plane, sometimes written as ρ, i.e., $\rho_m = a(1 - \epsilon^2)/(1 - \epsilon^2 \sin^2\phi)^{3/2}$

ρ_p = principal radius of curvature in the vertical east-west plane, called the prime radius of curvature and sometimes written as η, i.e., $\rho_p = a/(1 - \epsilon^2 \sin^2\phi)^{1/2}$

By resolving these equations into platform axes and performing some algebraic manipulation,

$$\left.\begin{aligned}\omega_{x_1} &= \frac{-V_{x_2}}{\rho_\alpha + h} + \frac{V_{x_1}\sin 2\alpha}{2}\,\frac{\rho_\rho - \rho_m}{(\rho_\rho + h)(\rho_m + h)}\\ \omega_{x_2} &= \frac{V_{x_1}}{\rho_{\alpha+90} + h} - \frac{V_{x_2}\sin 2\alpha}{2}\,\frac{\rho_\rho - \rho_m}{(\rho_\rho + h)(\rho_m + h)}\end{aligned}\right\} \tag{3}$$

where

ρ_α = radius of curvature at an azimuth $\alpha(1/\rho_\alpha) = (\sin^2\alpha/\rho_\rho) + (\cos^2\alpha/\rho_m)$

$\rho_{\alpha+90}$ = radius of curvature at an azimuth $\alpha + 90°$

$\rho_\rho - \rho_m = (a\epsilon^2 \cos^2\phi)/(1 - \epsilon^2 \sin^2\phi)^{3/2}$
$= [\epsilon^2/(1 - \epsilon^2)]\rho_m \cos^2\phi$

Equations (3) are the exact expressions for the torque rates of the platform relative to earth. The inertial torque rate is $\bar{\omega}_{EP} + \bar{\Omega} = \bar{\omega}_{IP}$. These are not power series approximations.

Note that the torque rate about the x_1 axis is not merely the x_2 component of velocity divided by the radius of curvature in the $x_2 - x_3$ plane except at cardinal headings. At all other headings, a small correction, proportional to V_{x1}, must be added. This correction is of the order $(\epsilon^2/2)(V/a)$, or about 0.1 deg/hr at 1800 knots. In geometric terms, the platform rotates around the velocity vector as well as around the binormal.

Equations (3) can be expanded in a power series in (h/a) and ϵ, which is accurate to $10^{-4}\,\Omega(0.0015$ deg/hr) for speeds up to 1800 knots and at altitudes below 25 naut miles:

$$\left.\begin{aligned}\omega_{x_1} &= -\frac{V_{x_2}}{a}\left[1 - \frac{h}{a} - \epsilon^2\left(\frac{\sin^2\phi}{2} - \cos^2\phi\cos^2\alpha\right)\left(1 - \frac{2h}{a}\right)\right] + \frac{V_{x_1}}{a}\frac{\epsilon^2}{2}\sin 2\alpha\cos^2\phi\\ \omega_{x_2} &= \frac{V_{x_1}}{a}\left[1 - h/a - \epsilon^2\left(\frac{\sin^2\phi}{2} - \cos^2\phi\sin^2\alpha\,(1 - 2\frac{h}{a})\right)\right] - \frac{V_{x_2}}{a}\frac{\epsilon^2}{2}\sin 2\alpha\cos^2\phi\end{aligned}\right\} \tag{4}$$

The calculation of position from the three components of velocity, as found in Eq. (1), depends on the coordinate frame chosen. For example, if $\alpha = 0$ so that the platform is north-seeking, then the latitude ϕ and longitude λ can be found from

$$\phi = \int_0^t \frac{V_{x_2}}{\rho_m + h}\,dt$$

$$\lambda = \int_0^t \frac{V_{x_1}}{(\rho_\rho + h)\cos\phi}\,dt$$

References

[1] Pitman, G. R. (ed.), *Inertial Guidance* (John Wiley and Sons Inc., New York, 1962), p. 149.

Shock Detachment Distance for Blunt Bodies in Argon at Low Reynolds Number

A. B. Bailey* and W. H. Sims†
ARO Inc., Arnold Air Force Station, Tenn.

Nomenclature

M_∞ = freestream Mach number
R_b = body radius (≡ nose radius of curvature for a sphere)
Re_2 = Reynolds number based on body diameter and conditions immediately downstream of a normal shock
T_0 = reservoir temperature of gas
T_w = body wall temperature
Δ = shock detachment distance measured from the body to the shock leading edge along the axis of symmetry

THE shock detachment distance in front of blunt bodies at high Reynolds numbers has been studied both theoretically and experimentally. Van Dyke and Gordon[1] have presented a theoretical analysis for a series of perfect gases having specific heat ratios of 1, $\frac{7}{5}$, and $\frac{5}{3}$ and a Mach number range from 1.2 to infinity. For a sphere, their analysis indicates that the shock detachment distance is primarily a function of the density ratio across the normal part of the shock. In such studies, it is implied that the shock and boundary-layer thicknesses are small compared with the shock detachment distance. At low Reynolds numbers the shock and boundary-layer thicknesses are no longer negligible, and at sufficiently low Reynolds numbers the shock and boundary layers merge. This implies that there must be a Reynolds number below which the shock detachment distance becomes a function of Reynolds number as well as density ratio.

Probstein and Kemp,[2] Ho and Probstein,[3] and Levinsky and Yoshihara,[4] among others, have analyzed this problem. All of these analyses indicate that as the fully merged regime is approached the shock detachment distance increases to a value greater than the inviscid value.

The low-density, hypervelocity (LDH) wind tunnel,[5] in operation at the von Kármán Gas Dynamics Facility of the Arnold Engineering Development Center, is well suited for low Reynolds number shock detachment distance investigations. When this tunnel is operated using argon, there is a natural flow visualization thought to be caused by radia-

Received September 3, 1963. This work was sponsored by Arnold Engineering Development Center, Air Force Systems Command, U. S. Air Force, under Contract No. AF 40(600)-1000.

* Engineer, Research Branch, von Kármán Gas Dynamics Facility.

† Engineer, Research Branch, von Kármán Gas Dynamics Facility. Member AIAA.

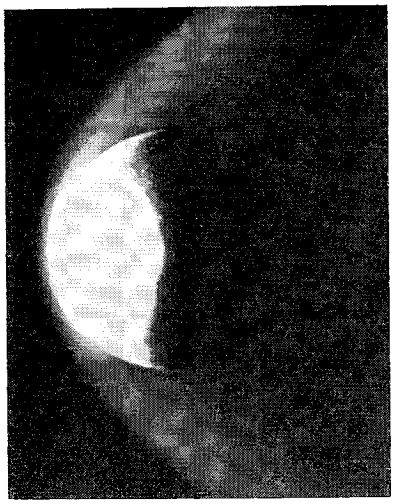

Fig. 1 Flow over a sphere in argon ($M_\infty = 6.23$, $T_0 = 2990°K$, $Re_2/in. = 334$, $R_b = 0.344$ in.).

tion from relaxing metastable argon atoms. This natural glow enables the shock shapes in front of bodies to be seen and photographed. A complete description of the tunnel operating conditions and the models used in this study may be found in a test report.[6]

The camera used was a standard 4 × 5 Speed Graphic, with a 13-in. focal length lens that could be stopped down to f5.6 mounted outside of the wind tunnel. A trial-and-error procedure established that good pictures could be obtained with Kodalith ASA 2 film with the lens stopped down to f5.6 and with exposure times ranging between 2 and 4 sec dependent upon the model position in the stream. A typical photograph is shown in Fig. 1. It is assumed in the present analysis that the leading edge of the shock is defined by the point at which the film density starts to increase. A photodensitometer was used to determine the point at which the film density increased, both on the body centerline and also at several off-axis stations. The advantage of this method was that it defined the shock shape with respect to the body and permitted greater accuracy in the determination of the shock detachment distance than would be possible with a single measurement on the axis of symmetry. It is considered that the maximum error involved in the present tests is ±10% for the smallest spheres tested.

In Fig. 2 the results of the determination of the shock detachment distance for spheres and flat-faced bodies are plotted in the form Δ/R_b vs Re_2. These curves show the dependence of shock detachment distance on body shape, Reynolds number, and Mach number.

Both shock-wave thickness and boundary-layer thickness at the stagnation point may be estimated.[7, 8] In the range of Reynolds numbers considered herein, both thicknesses are of the order of the detachment distance. In view of

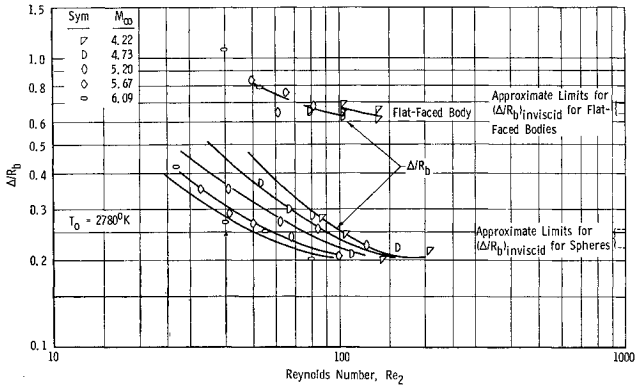

Fig. 2 Stagnation region shock detachment distance for a water-cooled sphere and flat-faced body in argon ($T_w/T_0 \simeq 0.11$).

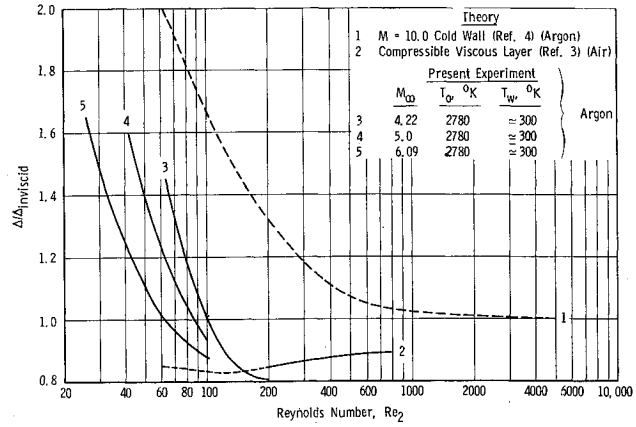

Fig. 3 Comparison of theoretical and experimental shock detachment distances.

this, it must be concluded that most of the results of this test are in the fully merged layer regime. It is of interest to note that the Reynolds number at which Δ/R_b is a minimum for spheres is in good agreement with the Reynolds number at which the impact pressure measured with a hemispherical-nosed probe is also a minimum.[9]

A method of correlating the present results with those obtained for other flow conditions is suggested by Stoddard,[10] where $(\Delta/R_b)/(\Delta/R_b)_{inviscid}$ is plotted against Re_2. Experimental values of $(\Delta/R_b)_{inviscid}$ for spheres in argon are given by Schwartz and Eckerman.[11] Using this parameter, the present results and the theoretical analyses of Refs. 3 and 4 are compared in Fig. 3. It will be noted that the decrease in the shock detachment distance to a value less than the inviscid value as predicted by Ho and Probstein is qualitatively confirmed in that some measured values of $(\Delta/R_b)/(\Delta/R_b)_{inviscid}$ are less than unity.

References

[1] Van Dyke, M. D. and Gordon, H. D., "Supersonic flow past a family of blunt axisymmetric bodies," NASA TR R-1 (1959).

[2] Probstein, R. F. and Kemp, N. H., "Viscous aerodynamic characteristics in hypersonic rarefied gas flow," J. Aerospace Sci. **27**, 174–192, 218 (1960).

[3] Ho, H.-T. and Probstein, R. G., "The compressible viscous layer in rarefied hypersonic flow," Brown Univ., ARL-TN-60-132 (1961).

[4] Levinsky, E. S. and Yoshihara, H., "Rarefied hypersonic flow over a sphere," *ARS Progress in Astronautics and Rocketry: Hypersonic Flow Research* (Academic Press, New York, 1962), Vol. 7, pp. 81–106.

[5] Potter, J. L., Kinslow, M., Arney, G. D., Jr., and Bailey, A. B., "Description and preliminary calibration of a low-density hypervelocity wind tunnel," Arnold Eng. Dev. Center TN-61-83 (August 1961).

[6] Bailey, A. B. and Sims, W. H., "The shock shape and shock detachment distance for spheres and flat-faced bodies in low-density, hypervelocity, argon flow," Arnold Eng. Dev. Center TDR-63-21 (February 1963).

[7] Ziering, S., Ek, F., and Koch, P., "Two-fluid model for the structure of neutral shock waves," Phys. Fluids **4**, 975–987 (1961).

[8] Cohen, C. B. and Reshotko, E., "The compressible laminar boundary layer with heat transfer and arbitrary pressure gradient," NACA Rept. 1294 (1956).

[9] Potter, J. L. and Bailey, A. B., "Pressure in the stagnation regions of blunt bodies in the viscous-layer to merged-layer regimes of rarefied flow," Arnold Eng. Dev. Center TDR-63-168 (July 1963).

[10] Stoddard, F. J., "Stagnation point viscous hypersonic flow," J. Aerospace Sci. **29**, 1138–1139 (1962).

[11] Schwartz, R. N. and Eckerman, J., "Shock location in front of a sphere as a measure of real gas effects," J. Appl. Phys. **27**, 169–174 (1956).